

Cosmological dynamics of scalar fields with $O(N)$ symmetry

Jian-gang Hao and Xin-zhou Li

Shanghai United Center for Astrophysics(SUCA), Shanghai Normal University,
Shanghai 200234, China
E-mail: kychz@shnu.edu.cn

Abstract. In this paper, we study the cosmological dynamics of scalar fields with $O(N)$ symmetry in general potentials. We compare the phase space of the dynamical systems of the quintessence and phantom and give the conditions for the existence of various attractors as well as their cosmological implications. We also show that the existence of tracking attractor in $O(N)$ phantom models require the potential with $\Gamma < 1/2$, which makes the model with exponential potential possess no tracking attractor.

PACS numbers: 0440-b, 9880Cq, 9880Es

1. Introduction

Astronomical measurements from Supernovae [1, 2, 3] and CMB anisotropy [4, 5, 6] independently confirm that about two-thirds of the energy density in our Universe is dark energy, which has negative pressure and accelerates the expansion of the Universe. The most widely studied models for dark energy are cosmological constant and a time varying scalar field with positive or negative kinetic energy evolving in a specific potential, referred to as "quintessence" with $w > -1$ [7, 8, 9, 10, 11, 12] and "phantom" with $w < -1$ [13, 14, 15, 16, 17] respectively. Since current observational constraint on the equation of state of the dark energy lies in the range $-1.38 < w < -0.82$ [18], it is still too early to rule out any of the above candidates. Complex scalar field as quintessence has been proposed in [19, 20] and its generalization to the scalar fields with $O(N)$ symmetry as quintessence and phantom in exponential potential have been done in [21, 22]. To study the global property of the cosmological system containing dark energy, phase space analysis is proved to be a powerful tool. For real scalar field quintessence and phantom models in FRW Universe, the phase space analysis have been done in [23, 24, 25, 26] while the analysis has been extended to the $O(N)$ scalar fields in exponential potentials in Ref.[21, 22]. In exponential potential, it has been show that the $O(N)$ phantom does not admit tracking attractor that plays an important role in alleviating the fine-tuning problem. In this paper, we study the phase space structure

of the scalar fields with $O(N)$ symmetry in general potentials and discuss the various attractors as well as the conditions for their stability.

2. Phase space of quintessence with $O(N)$ symmetry in general potentials

In this section, we study the phase space of quintessence with $O(N)$ symmetry in flat FRW cosmological background

$$ds^2 = dt^2 - a^2(t)d\mathbf{x}^2 \quad (1)$$

The corresponding equations of motion as well as Einstein equations are just a simple generalization of those for exponential potential as shown in [21].

$$\begin{aligned} \dot{H} &= -\frac{\kappa^2}{2}(\rho_\gamma + p_\gamma + \dot{R}^2 + \frac{\Sigma^2}{a^6 R^2}) \\ \dot{\rho}_\gamma &= -3H(\rho_\gamma + p_\gamma) \\ \ddot{R} + 3H\dot{R} - \frac{\Sigma^2}{a^6 R^3} + V'(R) &= 0 \\ H^2 &= \frac{\kappa^2}{3}[\rho_\gamma + \frac{1}{2}(\dot{R}^2 + \frac{\Sigma^2}{a^6 R^2}) + V(R)] \end{aligned} \quad (2)$$

where R is the radial component of the scalar fields with $O(N)$ symmetry and all "angular" equations have been integrated out and their contributions to the system is reflected by the terms associated with Σ , the integration constant of "angular" equations [21]. ρ_γ and p_γ are the energy density and pressure of the baryotropic matter and $p_\gamma = (\gamma - 1)\rho_\gamma$, where γ is a constant, $0 \leq \gamma \leq 2$. Here, we denote $\kappa^2 = 8\pi G$. Now, introducing the following variables: $x = \frac{\kappa\dot{R}}{\sqrt{6}H}$, $y = \frac{\kappa\sqrt{V(R)}}{\sqrt{3}H}$, $z = \frac{\kappa}{\sqrt{6}H}\frac{\Sigma}{a^3 R}$, $\xi = \frac{1}{\kappa R}$, $\lambda = -\frac{V'(R)}{\kappa V(R)}$, $\Gamma = \frac{V(R)V''(R)}{V'^2(R)}$ and $N = \log a$, the equation system(2) becomes the following autonomous system:

$$\begin{aligned} \frac{dx}{dN} &= \frac{3}{2}x[\gamma(1 - x^2 - y^2 - z^2) + 2(x^2 + z^2)] - (3x - \sqrt{6}z^2\xi - \sqrt{\frac{3}{2}}\lambda y^2) \\ \frac{dy}{dN} &= \frac{3}{2}y[\gamma(1 - x^2 - y^2 - z^2) + 2(x^2 + z^2)] - \sqrt{\frac{3}{2}}\lambda xy \\ \frac{dz}{dN} &= -3z + \frac{3}{2}z[\gamma(1 - x^2 - y^2 - z^2) + 2(x^2 + z^2)] - \sqrt{6}xz\xi \\ \frac{d\xi}{dN} &= -\sqrt{6}\xi^2x \\ \frac{d\lambda}{dN} &= -\sqrt{6}\lambda^2x(\Gamma - 1) \end{aligned} \quad (3)$$

Now, it is straightforward to analyze the critical points as well as their stability. In **table 1**, we list the stable critical points, conditions for their existence and the cosmological parameters there (Note that we have omitted those unstable critical points). We include a detailed analysis for the tracking attractor and the corresponding eigenvalues of the linear perturbation matrix in **Appendix A** and **B**.

| Critical points (x,y,z, ξ) | Name | Conditions | Ω_R | w_R |
|--|------------------------|--|-------------------------------|----------------------------|
| $\frac{\lambda}{\sqrt{6}}, \sqrt{1 - \frac{\lambda^2}{6}}, 0, 0$ | quintessence attractor | $\Gamma = 1, \lambda \neq 0, \lambda^2 < 3\gamma$ | 1 | $-1 + \frac{\lambda^2}{3}$ |
| $\sqrt{\frac{3}{2}} \frac{\gamma_e}{\lambda}, \sqrt{\frac{3\gamma_e(2-\gamma_e)}{2\lambda^2}}, 0, 0$ | tracking attractor | $\Gamma > \frac{1}{2}, \lambda \neq 0, \gamma_e < 2$ | $\frac{3\gamma_e}{\lambda^2}$ | $\gamma_e - 1$ |
| 0,1,0,0 | de Sitter attractor | $\lambda = 0$ | 1 | -1 |

Table 1. The critical points and their physical properties for $O(N)$ quintessence model. Here, $\gamma_e \equiv \frac{\gamma}{2\Gamma-1}$. Considering the requirements $\gamma_e < 2$ and $\Gamma > \frac{1}{2}$ together, we have $\Gamma > \frac{\gamma/2+1}{2}$ for the stability of the attractor.

3. Phase space of phantom with $O(N)$ symmetry in general potentials

Phantom with $O(N)$ symmetry in exponential potential has been proposed in Ref.[22]. However, in exponential potential, the tracking attractor does not exist and thus make the model need careful fine-tuning. In this section, we will consider the model in a general potential and give a condition for the existence of tracking attractor. In flat FRW spacetime, the equations of motion as well as Einstein equations are

$$\begin{aligned} \dot{H} &= -\frac{\kappa^2}{2}(\rho_\gamma + p_\gamma - \dot{R}^2 - \frac{\Sigma^2}{a^6 R^2}) \\ \dot{\rho}_\gamma &= -3H(\rho_\gamma + p_\gamma) \\ \ddot{R} + 3H\dot{R} - \frac{\Sigma^2}{a^6 R^3} - V'(R) &= 0 \\ H^2 &= \frac{\kappa^2}{3}[\rho_\gamma - \frac{1}{2}(\dot{R}^2 + \frac{\Sigma^2}{a^6 R^2}) + V(R)] \end{aligned} \quad (4)$$

By using the same dimensionless parameters as defined in previous section, we can reduce the equation system (4) to

$$\begin{aligned} \frac{dx}{dN} &= \frac{3}{2}x[\gamma(1 + x^2 - y^2 + z^2) - 2(x^2 + z^2)] - (3x - \sqrt{6}z^2\xi + \sqrt{\frac{3}{2}}\lambda y^2) \\ \frac{dy}{dN} &= \frac{3}{2}y[\gamma(1 + x^2 - y^2 + z^2) - 2(x^2 + z^2)] - \sqrt{\frac{3}{2}}\lambda xy \\ \frac{dz}{dN} &= -3z + \frac{3}{2}z[\gamma(1 + x^2 - y^2 + z^2) - 2(x^2 + z^2)] - \sqrt{6}xz\xi \\ \frac{d\xi}{dN} &= -\sqrt{6}\xi^2x \\ \frac{d\lambda}{dN} &= -\sqrt{6}\lambda^2x(\Gamma - 1) \end{aligned} \quad (5)$$

By comparing the dynamical system of $O(N)$ phantom Eqs.(4) with $O(N)$ quintessence Eqs.(2), one can find that their differences are merely the sign difference of the terms associated with kinetic energy. However, these small changes make their dynamics quite different. In **table 2**, we list the critical points, conditions of existence and stability as well as cosmological parameters there for $O(N)$ phantom in general potentials. We

| Critical points (x,y,z, ξ) | Name | Conditions | Ω_R | w_R |
|--|---------------------|--|--------------------------------|----------------------------|
| $-\frac{\lambda}{\sqrt{6}}, \sqrt{1 + \frac{\lambda^2}{6}}, 0, 0$ | big rip attractor | $\Gamma = 1, \lambda \neq 0, \lambda^2 < 3\gamma$ | 1 | $-1 - \frac{\lambda^2}{3}$ |
| $\sqrt{\frac{3}{2}} \frac{\gamma_e}{\lambda}, \sqrt{\frac{3\gamma_e(\gamma_e-2)}{2\lambda^2}}, 0, 0$ | tracking attractor | $\Gamma < \frac{1}{2}, \lambda \neq 0, \gamma_e < 2$ | $-\frac{3\gamma_e}{\lambda^2}$ | $\gamma_e - 1$ |
| 0,1,0,0 | de Sitter attractor | $\lambda = 0$ | 1 | -1 |

Table 2. The critical points and their physical properties for $O(N)$ phantom model. Here, $\gamma_e \equiv \frac{\gamma}{2\Gamma-1}$

need to emphasize that in exponential potential, the $O(N)$ phantom model does not admit tracking attractor solution[22]. This is due the fact that the existence of tracking attractor requires that the potentials must have $\Gamma < 1/2$ while the exponential potential with $\Gamma = 1$ is excluded. Another important point of $O(N)$ phantom lies in that the existence of stable big rip attractor requires $\lambda^2 < 3\gamma$, which therefore impose a lower bound to the equation of state $w > -1 - \gamma$. The similar property $w < -1 + \gamma$ also hold for the $O(N)$ quintessence case but the significance is less because this upper bound won't be much physical interest.

From the above qualitative analysis, we need to stress that the critical point structure is unchanged from the single-field when the internal $O(N)$ symmetry is introduced since the critical points correspond to vanishing angular components ($z = 0$). However, the angular component will definitely affect the trajectories approaching the critical points which we will explore in the ensuing section.

4. Numerical analysis of the $O(N)$ quintessence and phantom

In previous sections, we have studied the phase space of scalar field with $O(N)$ symmetry in a flat FRW cosmological background. The critical points indicate that these stable attractor phases corresponding to the vanishing of "angular" components resulted from the $O(N)$ symmetry. Thus, what will be the effects of the $O(N)$ symmetry? In fact, the introduction of the "angular" term will change the evolutionary tracks of the dynamical systems, which was not well manifested by the above qualitative analysis. In this section, we study their dynamical evolution numerically and compare the results with the cases of real scalar field models. Here, we choose the potential as the power law of the field $V(R) = V_0(R_0/R)^q$. We choose $q = 4$ and $q = -5/4$ for $O(N)$ quintessence and phantom with corresponding $\Gamma = 5/4$ and $\Gamma = 1/5$. The parameters were chosen as $V_0 = 0.00001$, $R_0 = H_0 = \kappa = 1$ and $\Sigma = 15$.

From Fig.1 to Fig.4, we plot the dynamical evolution of matter, radiation and dark energy be it quintessence or phantom with or without $O(N)$ symmetry. Comparing Fig.1 and Fig.2 as well as Fig.3 and Fig.4, one can find that the internal symmetry will affect the dynamical evolution at very early epoch. The early property of quintessence or phantom will definitely affect the CMB spectrum and thus provide the possibility that how to discriminate them from their counterpart without $O(N)$ symmetry. Especially,

for $O(N)$ quintessence, the energy density is not necessarily negligible compared to radiation and matter due to the contribution of "angular" term that is proportional to a^{-6} , which allows a non-negligible energy density for dark energy at early epoch. This is a very interesting feature because if the dark energy is cosmological constant, its initial energy density need to be some 100 orders of magnitude or smaller than the initial matter-energy density [27] and thus pose the fine-tuning problem and coincidence problem. While in $O(N)$ quintessence, the "angular" term will contribute a kinetic energy that decrease very fast as the universe expands (proportional to a^{-6}). So, the initial energy condition could be comparable to the matter which is more natural than the real scalar field models.

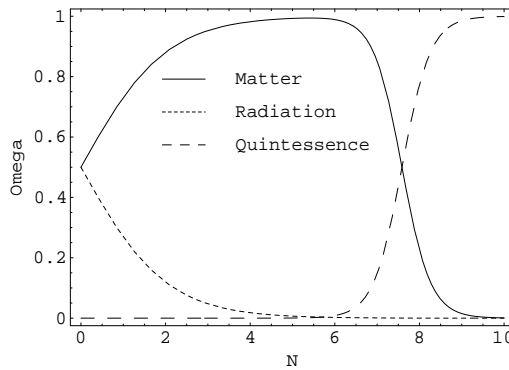


Figure 1. Evolution of cosmic parameters for matter, radiation and quintessence without $O(N)$ symmetry. The plot begins with $\Omega_{m,i} = \Omega_{r,i} = 0.499$ and $\Omega_R = 0.002$. Note also that the label N of horizontal axis has nothing to do with the $O(N)$ symmetry, it is the e-fold number defined as $N = \ln a$.

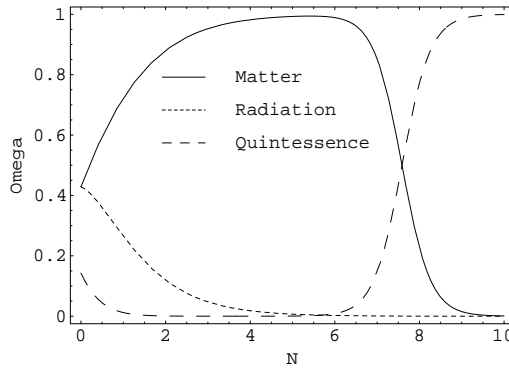


Figure 2. Evolution of cosmic parameters for matter, radiation and quintessence with $O(N)$ symmetry. The tilt of the curve at the early epoch is an important feature of $O(N)$ quintessence. The plot begins with $\Omega_{m,i} = \Omega_{r,i} = 0.425$ and $\Omega_R = 0.150$

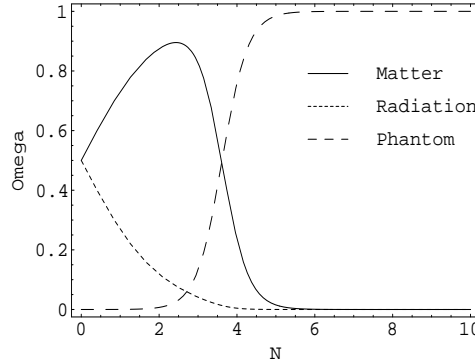


Figure 3. Evolution of cosmic parameters for matter, radiation and phantom without $O(N)$ symmetry. The plot begins with $\Omega_{m,i} = \Omega_{r,i} = 0.499$ and $\Omega_R = 0.002$

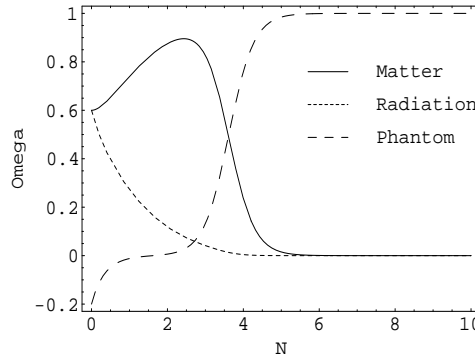


Figure 4. Evolution of cosmic parameters for matter, radiation and phantom with $O(N)$ symmetry. To make the difference between the $O(N)$ phantom and phantom clearer, we allow a negative Ω_R at the initial part, which by definition is positive. In fact, in a realistic model, the initial values should be chosen with respect to the energy condition $\rho \geq 0$ and the result will be that all curves will go upwards.

5. Discussion and Conclusion

In this paper, we study the cosmological dynamics of scalar field with $O(N)$ symmetry in general potentials. We show that although there are merely several sign differences between the $O(N)$ phantom and quintessence system, the dynamical evolution, the phase space property and the physical significance are quite different, which lead to the difference requirements for the potentials to admit stable tracking attractors. This requirement for $O(N)$ phantom, i.e. $\Gamma < 1/2$ makes the exponential potential with $\Gamma = 1$ admit no tracking attractor, which is in agreement with the conclusion obtained in Ref.[22]. Another important point we need to stress is that in the phantom model, the stability of big rip attractor requires that the resulting equation of state $w > -1 - \gamma$, which has very interesting physical implication because this may add a natural priori for the lower bound of w and plays a very important role in data analysis of SNeIa[3]. We

also show that for the $O(N)$ quintessence model, the initial energy density could be larger and won't affect the evolution too much because the "angular" kinetic energy decreases with a^{-6} . In real scalar field quintessence, tracker mechanism was used to provide a non-negligible energy density at early epoch. In the $O(N)$ quintessence model, if equipped with the same tracker mechanism, it will admit a wider range of initial energy density.

Appendix A. Analysis for Tracking attractors of $O(N)$ quintessence and phantom

In this appendix, we show the way to analyze the tracking attractors in the dynamical systems of $O(N)$ quintessence and phantom. From the dynamical system listed in **section 2** and **3**, one can not identify tracking attractors. The tracking attractors listed in **Table 1** and **Table 2** are obtained through the following analysis. The tracking attractors exist when λ is very large and $\Gamma \simeq \text{constant}$. So, we introduce the following dimensionless variables re-scaled by $\epsilon \equiv \frac{1}{\lambda}$. These variables are $X = x/\epsilon$, $Y = y/\epsilon$, $Z = z/\epsilon$ and $\Theta = \xi/\epsilon$ with x , y , z and ξ defined in **section 2**. Then the dynamical system could be rewritten as

$$\begin{aligned} \frac{dX}{dN} &= -\sqrt{6}X^2(\Gamma - 1) + \frac{3}{2}\gamma X - 3X \pm \sqrt{\frac{3}{2}}Y^2 & (A.1) \\ \frac{dY}{dN} &= -\sqrt{6}XY(\Gamma - 1) + \frac{3}{2}\gamma Y - \sqrt{\frac{3}{2}}XY \\ \frac{dZ}{dN} &= -\sqrt{6}XY(\Gamma - 1) + \frac{3}{2}\gamma Z - 3Z \\ \frac{d\Theta}{dN} &= -\sqrt{6}X\Theta(\Gamma - 1) \end{aligned}$$

where the plus and minus signs of the last term of the first equation correspond to quintessence and phantom respectively. Also, we have dropped the terms containing the small quantity ϵ in Eqs.(A.1). Now, it will be straightforward to obtain the critical points of the above equation system (A.1) by setting the righthand sides to zero. The results are contained in **table 1** and **table 2**. It is worth noting that the equations for $O(N)$ quintessence and for $O(N)$ phantom are very similar with only a sign difference of one term. However, this small change lead to very different expressions for the cosmic density parameters at the tracking attractors, i.e. $\frac{3\gamma_e}{\lambda^2}$ and $-\frac{3\gamma_e}{\lambda^2}$ for quintessence and phantom respectively. These expressions indicate that γ_e for $O(N)$ phantom must be negative so that the corresponding Ω_R makes sense and thus requires that Γ of the potential must be less than 1/2. From the definition of Γ , it would be clear that exponential potential has $\Gamma = 1$ and therefore won't admit tracking attractor in phantom dynamical system.

Appendix B. The eigenvalues of the linear perturbation matrix for different stable critical points

To determine the stability, we need to linearize the corresponding equation system (3), (5) and (A.1) in a neighborhood of the critical points, and then determine the stability of the systems by the eigenvalues of the coefficients matrix. By this way, we calculated the various eigenvalues corresponding to each critical points and tabulated the results in **table B1** and **table B2**. We need to point out that the eigenvalues for tracking attractors of $O(N)$ quintessence and phantom are the same to each other because the linearized equations have only one sign-different term, see Eqs.(A.1) and this difference just does not enter into the corresponding eigenvalues coincidentally. From the eigenvalues, we obtain the condition for the stability of the critical points, which is contained in **Table 1** and **Table 2**. Note that the eigenvalues for the tracking attractors are very complicated, and thus we compute them for the power law potential as we have used in **section 4**. The results are listed in **Table B3**, from which we know that the tracking attractors are stable.

| Critical points (x, y, z, ξ) | eigenvalues |
|--|---|
| $\frac{\lambda}{\sqrt{6}}, \sqrt{1 - \frac{\lambda^2}{6}}, 0, 0$ | $0, \frac{1}{2}(\lambda^2 - 6), \frac{1}{2}(\lambda^2 - 6), \lambda^2 - 3\gamma$ |
| $\sqrt{\frac{3}{2}}\gamma_e, \sqrt{\frac{3\gamma_e(2-\gamma_e)}{2}}, 0, 0$ | $-3(\Gamma - 1)\gamma_e, \frac{-3(2+(2\Gamma-3)\gamma_e)}{4}[1 + \frac{\sqrt{4+(4-24\Gamma)\gamma_e+(1+2\Gamma)^2\gamma_e^2}}{2+(2\Gamma-3)\gamma_e}]$ $\frac{3}{2}(\gamma_e - 2), \frac{-3(2+(2\Gamma-3)\gamma_e)}{4}[1 - \frac{\sqrt{4+(4-24\Gamma)\gamma_e+(1+2\Gamma)^2\gamma_e^2}}{2+(2\Gamma-3)\gamma_e}]$ |
| $0, 1, 0, 0$ | $-3, -3, 0, -3\gamma$ |

Table B1. The eigenvalues of the critical points for $O(N)$ quintessence. Note that the critical point for the tracking attractor (the second row) as well as its corresponding eigenvalues are given in terms of (X, Y, Z, Θ)

| Critical points (x, y, z, ξ) | eigenvalues |
|--|---|
| $\frac{-\lambda}{\sqrt{6}}, \sqrt{1 + \frac{\lambda^2}{6}}, 0, 0$ | $0, \frac{1}{2}(-\lambda^2 - 6), \lambda^2 - 3\gamma, \frac{1}{2}(\lambda^2 - 6)$ |
| $\sqrt{\frac{3}{2}}\gamma_e, \sqrt{\frac{3\gamma_e(\gamma_e-2)}{2}}, 0, 0$ | $-3(\Gamma - 1)\gamma_e, \frac{-3(2+(2\Gamma-3)\gamma_e)}{4}[1 + \frac{\sqrt{4+(4-24\Gamma)\gamma_e+(1+2\Gamma)^2\gamma_e^2}}{2+(2\Gamma-3)\gamma_e}]$ $\frac{3}{2}(\gamma_e - 2), \frac{-3(2+(2\Gamma-3)\gamma_e)}{4}[1 - \frac{\sqrt{4+(4-24\Gamma)\gamma_e+(1+2\Gamma)^2\gamma_e^2}}{2+(2\Gamma-3)\gamma_e}]$ |
| $0, 1, 0, 0$ | $-3, -3, 0, -3\gamma$ |

Table B2. The eigenvalues of the critical points for $O(N)$ phantom. Note that, similar to the case in Table B1, the critical point for the tracking attractor (the second row) as well as its corresponding eigenvalues are given in terms of (X, Y, Z, Θ)

| Models | Γ | γ | γ_e | $Re(\lambda_1)$ | $Re(\lambda_2)$ |
|-----------------------|----------|----------|------------|-----------------|-----------------|
| O(N) quintessence | 5/4 | 4/3 | 8/9 | -1.1667 | -1.1667 |
| | | 1 | 2/3 | -1.2500 | -1.2500 |
| O(N) phantom | 1/5 | 4/3 | -20/9 | -8.7820 | -2.8847 |
| | | 1 | -5/3 | -7.2122 | -2.2878 |

Table B3. The numerical results of the real part of the eigenvalues for the tracking attractors when the background fluid is radiation $\gamma = 4/3$ and matter $\gamma = 1$ in the power law potential as we described in **section 4**.

Acknowledgments

This work is supported by NKBRSP under Grant No. 1999075406.

References

- [1] Riess A G *et al.* 1998 *Astron. J.* **116** 1009
- [2] Perlmutter S *et al.* 1999 *Astrophys. J.* **517** 565
- [3] Tonry J L *et al.* 2003 *Astrophys. J.* **594** 1
- [4] Bennett C L *et al.* *Astrophys. J. Suppl.* **148** 1
- [5] Netterfield C B *et al.* 2002 *Astrophys. J.* **517** 604
- [6] Halverson N W *et al.* 2002 *Astrophys. J.* **568** 38
- [7] Ratra B and Peebles P J 1988 *Phys. Rev.* **D37** 3406
- [8] Wetterich C 1988 *Nucl. Phys.* **B302** 668
- [9] Ferreira P and Joyce M 1997 *Phys. Rev. Lett.* **79** 4740
- [10] Coble K, Dodelson S and Frieman J 1997 *Phys. Rev.* **D55** 1851
- [11] Caldwell R R, Dave R and Steinhardt P J 1998 *Phys. Rev. Lett.* **80** 1582
- [12] Peebles P J E, Ratra B 2003 *Rev. Mod. Phys.* **75** 599
Padmanabhan T 2003 *Phys. Rep.* **380** 235
- [13] Caldwell R R 2002 *Phys. Lett.* **B545** 23
- [14] Schulz A E and White M 2001 *Phys. Rev.* **D64** 043514
- [15] Carroll S M, Hoffman M and Trodden M 2003 *Phys. Rev.* **D68** 023509
- [16] Hao J G and Li X Z 2003 *Phys. Rev.* **D67** 107303
Hao J G and Li X Z 2003 *Phys. Rev.* **D68** 043501
- [17] Singh P, Sami M and Dadhich N 2003 *Phys. Rev.* **D68** 023522
- [18] Melchiorri A, Mersini L, Odman C J and Trodden M 2003 *Phys. Rev.* **D68** 043509
- [19] Gu J A and Huang W Y 2001 *Phys. Lett.* **B517** 1
- [20] Boyle L A, Caldwell R R and Kamionkowski M 2002 *Phys. Lett.* **B545** 17
- [21] Li X Z, Hao J G and Liu D J 2002 *Class. Quant. Grav.* **19** 6049
- [22] Li X Z and Hao J G 2004 *Phys. Rev.* **D69** 107303
- [23] Copeland E J, Liddle A R and Wands D 1998 *Phys. Rev.* **D57** 4686
- [24] Steinhardt P J, Wang L and Zlatev I 1999 *Phys. Rev.* **D59** 123504
- [25] Ng S C C, Nunes N J and Rosati F 2001 *Phys. Rev.* **D64** 083510
- [26] Hao J G and Li X Z 2003 *Preprint* astro-ph/0309746, To be published in *Phys. Rev. D*
- [27] Armendariz-Picon C, Mukhanov V and Steinhardt P J 2001 *Phys. Rev.* **D63** 103510